

Identifying Potential BO_2 Oxide Polymorphs for Epitaxial Growth Candidates

Prateek Mehta,[†] John R. Kitchin,^{*,†} and Paul A. Salvador[‡]

Department of Chemical Engineering, Carnegie Mellon University, 5000 Forbes Ave, Pittsburgh, PA 15213, and Department of Materials Science and Engineering, Carnegie Mellon University, 5000 Forbes Ave, Pittsburgh, PA 15213

E-mail: jkitchin@andrew.cmu.edu

Abstract

Transition metal dioxides (BO_2) exhibit a number of polymorphic structures with distinct properties, but the isolation of different polymorphs for a given composition is carried out using trial and error experimentation. We present computational studies of the relative stabilities and equations of state for six polymorphs (anatase, brookite, rutile, columbite, pyrite, and fluorite) of five different BO_2 dioxides ($\text{B} = \text{Ti}, \text{V}, \text{Ru}, \text{Ir}, \text{and Sn}$). These properties were computed in a consistent fashion using several exchange correlation functionals within the density functional theory formalism, and the effects of the different functionals are discussed relative to their impact on predictive synthesis. We compare the computational results to prior observations of high-pressure synthesis and epitaxial film growth, and then use this discussion to predict new accessible polymorphs in the context of epitaxial stabilization using isostructural substrates.

^{*}To whom correspondence should be addressed

[†]Department of Chemical Engineering, Carnegie Mellon University, 5000 Forbes Ave, Pittsburgh, PA 15213

[‡]Department of Materials Science and Engineering, Carnegie Mellon University, 5000 Forbes Ave, Pittsburgh, PA 15213

For example, the relative stabilities of the columbite polymorph for VO_2 and RuO_2 are similar to those of TiO_2 and SnO_2 , the latter two of which have been previously stabilized as epitaxial films.

1 Introduction

Oxides are technologically important materials for a wide range of applications ranging from catalysis (including CO oxidation¹⁻⁴ and photocatalysis^{5,6}), electrodes,^{7,8} sensors^{9,10} and electronic devices.^{11,12} Oxides often exhibit various polymorphic structures, but not all are stable in ambient or other easily accessible synthesis conditions. The metastable polymorphs are the subject of considerable interest due to their unique and sometimes superior chemical properties. TiO_2 , for example, exists naturally in the rutile and anatase polymorphs but anatase has significantly higher photocatalytic activity than rutile.^{13,14} As another example, RuO_2 in the modified fluorite structure (only accessible at high pressures) has been found to be very hard compared to the stable rutile polymorph.^{15,16} The metastable $\text{VO}_2(\text{B})$ polymorph has been recently shown to exhibit improved electrochemical performance in lithium-ion batteries compared to other well known vanadium polymorphs.¹⁷ Finding ways to synthesize specific polymorphs is of great interest for applications, and isolating methods to realize new polymorphs will open avenues for materials design.

The natural starting point for predicting which oxide polymorph can be synthesized is to establish the relative stabilities of all polymorphs at the synthesis conditions, where the lowest energy phase will be thermodynamically preferred. While it is well established that the kinetics required to form different polymorphic structures from a specific precursor state can often be manipulated to result in synthesis of metastable phases, the relative stability of kinetically accessible phases often fall within a fairly narrow range of energies. The relative stabilities of polymorphs can be directly modified if they are grown as thin films,¹⁸⁻²⁰ where the interfacial energies between the nucleus of different thin polymorph films and the substrate can cause reordering in their relative stabilities. In the case of TiO_2 ,

it is known that the (001) surfaces of single crystal perovskites favor the growth of anatase, while (111) surfaces favor the growth of rutile.^{21,22} For epitaxial stabilization, one also expects that the interfacial energy differences can only cause reordering of polymorphs within some energetic window, and an empirically plausible energy window is on the order of 1-10 kJ/mol (described later), though the true bounds for any given system are not well-known.

It is of great interest to expand the use of epitaxial stabilization methods for the development of broader classes of materials, such as complex structures or phases that do not compete as the lowest energy phase in pressure or temperature space, but still exist as local minima in free energy relative to other phases. One example where epitaxial stabilization has been successful in obtaining such a phase was in the synthesis of the hexagonal polymorph of SmMnO_3 which is stable (by 9 kJ/mol)²³⁻²⁵ at ambient pressure in the dense perovskite polymorph. A new high-throughput structural characterization method, combinatorial substrate epitaxy(CSE),^{26,27} that allows hundreds of film growth experiments to be carried out in parallel on easily fabricated polycrystalline substrates, has shown that such broad new classes of materials are accessible. A new polymorphic form of $\text{Dy}_2\text{Ti}_2\text{O}_7$ was found using CSE methods,²⁷ while single crystal approaches failed owing to kinetic barriers to accessing the lowest energy state.²⁸ The parallel nature of CSE also allowed enough observations to be made to demonstrate only a few competitive orientation relationships (ORs) actually exist between film-substrate pairs (regardless of substrate surface orientation), including for TiO_2 , Fe_2O_3 ,²⁹ and $\text{Ca}_3\text{Co}_4\text{O}_9$.³⁰ Though only one OR was observed per polymorph using CSE, phase stability of TiO_2 on BaTiO_3 and BiFeO_3 was orientation dependent: epitaxial anatase (rutile) was stable nearby to (far away from) (001)-oriented BiFeO_3 .^{26,31} Even though CSE is faster and less onerous than single crystal methods, the identification of potential synthesis candidates and the selection of suitable substrates and growth conditions is carried out by trial and error.

It would be beneficial to know which polymorphs are energetically close in stability, because these might be good candidates for epitaxial stabilization. Unfortunately, this in-

formation is difficult to come by experimentally. However, computations can be used to rapidly explore composition and structure space so that materials with desired properties can be identified and designed. This is a much used approach in the area of high-pressure research, where computational methods have been used to understand and predict materials stability as a function of pressure for many BO_2 oxides.^{32–34} In such work, the internal or free energies of competing polymorphs are computed versus volume, and this is used to rationalize synthetic procedures to obtain appropriate thermodynamic conditions for polymorph stability inversion. The same tools used in high-pressure phase exploration are applicable in the field of thin film growth. Simply generating libraries of formation energies for specific polymorphs helps guide the experimentalist towards high-probability targets based on the accessible range of interfacial energies that modify polymorph stability during growth (discussed in detail later).^{19,24,25,27,35} The principle idea is that polymorphs that are energetically close to the most stable state (i.e., within some energy window) are probable candidates for epitaxial stabilization. What is needed then are libraries of the relative stabilities of oxide polymorphs, which can be generated computationally. While other studies have compared the relative stabilities of different oxide polymorphs, the focus of these studies has been either the study of physical properties or the prediction of potential high pressure phases. Materials Genome approaches, like the Materials Project,³⁶ can also be used to compare relative stability of some polymorphs, but the current database does not contain all polymorphs of each oxide. In addition, the database does not currently include relevant information such as the equation of state or the bulk modulus, which can be used in simple free energy models to estimate relative stabilities at higher pressure and temperature.³⁷

In this work we have considered the anatase, rutile, brookite, columbite, fluorite, and pyrite polymorphs of five different BO_2 oxides: TiO_2 , VO_2 , RuO_2 , IrO_2 and SnO_2 . The equations of state and relative stabilities have been computed using several exchange-correlation functionals within the density functional theory formalism. The set of data calculated in this work has substantial value beyond simply estimating relative stability. Trends in stability

or band structures may be deduced, elastic properties can be estimated, and the structures may serve as starting points for other types of calculations in the future. For example, substrate-film interfacial energies and film surface energies can be computed in order to produce a complete picture of epitaxial stabilization. Volumetric free energies can also be used to study phase behavior at higher pressures and temperatures.³⁷ To facilitate maximal availability of this data, JSON (JavaScript Object Notation) libraries containing information such as volumes, energies, unit cell parameters, etc... as well as all of the computational parameters used for the calculations have been included in the supporting information³⁸ associated with this work along with examples of using this data.

The rest of this paper is organized as follows. In section 2, the technical details of the first principles calculations and methodology applied have been outlined. In section section 3, the results are presented and discussed, with a particular focus on describing an energetic window of opportunity for epitaxial stabilization of new compounds. Finally, in section 4, the conclusions of the work have been provided.

2 Methods

The DFT based first-principles calculations were performed using the Vienna ab-initio Simulation Package (VASP)^{39,40} using the projector-augmented wave pseudopotentials.^{41,42} The exchange correlational functionals used were the local gradient approximation (LDA),⁴³ and three different generalized gradient approximations: PBE,^{44,45} PBEsol⁴⁶ and AM05.^{47,48} To obtain high precision the plane wave cutoff energy was set to be 520 eV. For the Brillouin zone sampling, a k -point convergence study was performed for all polymorphs of all oxides to reach an energy convergence of 10 meV per formula unit. The Monkhorst-Pack k -point grids⁴⁹ used for the different structures are described in the supporting information.³⁸

Geometry optimization was performed in a three step process. In the first step, an appropriate range of volumes was found at constant shape and relaxed ions. In step two,

the atom positions were allowed to change at a series of fixed volumes. At this point, the internal energies and volumes for each structure were fit to the Birch-Murnaghan equation of state⁵⁰ to determine the equilibrium volume and bulk modulus. A final calculation was done near the minimum energy from step two, allowing the volume also to change to get the equilibrium unit cell parameters. The relative stabilities of each polymorph were evaluated at the equilibrium volume each polymorph.

3 Results and Discussion

Before analyzing individual polymorphs in greater detail, we discuss general trends in stability, how our data compares to literature and how the choice of exchange-correlation functional affects our results. In 3 - 7, discussed in detail later, the equilibrium energies of the polymorphs for each oxide have been plotted. In general, it is seen that rutile is the lowest energy polymorph for all oxides, with the exception of TiO_2 . There has been much debate about the most stable ambient condition TiO_2 polymorph, and this will be discussed in greater detail in section 3.1. The volume per formula unit is generally seen to vary as fluorite < pyrite < columbite < rutile < brookite < anatase. The bulk modulus generally has an inverse relation to volume shown in 1. The scatter in the $B(V)$ relationship arises both from variations owing to the specific functional used and differences in bonding across compositions. Anatase and brookite VO_2 polymorphs are observed to be outliers to the the linear trend. Possible reasons have been discussed in section 3.2. A comparison of some of the calculated volumes and bulk moduli to other experimental and theoretical works has been made in 1 and 2.

The exchange-correlation functionals show the expected behavior, with LDA underestimating the volume and PBE overestimating the volume (see 2). The AM05 and PBEsol volumes are very similar and lie between those for LDA and PBE. We have found that AM05 and PBEsol volumes most closely resemble experimental values. The choice of functional

also affects the relative stability. This effect is less pronounced for polymorphs of similar volume as compared to polymorphs with largely differing volumes, in which case there is more variation in the relative energies across functionals (seen in 3 - 7). For predictive synthesis, the variation across functionals can be used to put bounds on the maximum and minimum energy differences required for epitaxial stabilization to be successful.

Polymorphs close in energy to the lowest energy polymorph are targets for epitaxial synthesis, and compositions that exhibit narrow energy landscapes for multiple polymorphs, such as TiO_2 , are ideal candidates for epitaxial stabilization. Using a simple model to describe the energy difference between thin layers of two phases, we can estimate the range of stabilities accessible in epitaxial stabilization.

In free energy terms, the difference of interest is difference in formation energy between the two polymorphs as thin films: $\Delta G_{poly,films}$. This can be expressed as:^{24,35}

$$\Delta G_{poly,films} = V\Delta\Delta G_{V,bulk} + V\Delta w + A\Delta\gamma_{sub/film} + A\Delta\gamma_{surf}, \quad (1)$$

where V (A) is the volume (area) of the film (assuming flat surfaces), $\Delta\Delta G_{V,bulk}$ is the difference in the volumetric bulk formation energy, Δw is the volumetric strain energy difference between the polymorph films, and $\gamma_{sub/film}$ (γ_{surf}) is the specific film/substrate (film/vapor) interfacial energy. In the most robust versions of epitaxial stabilization, where polymorphs are stabilized via interfacial energies, the two largest terms in Eq. 1 are $V\Delta\Delta G_{V,bulk}$ and $A\Delta\gamma_{sub/film}$. To find a reasonable bound in energies to compare with DFT values, one can discard the negligible terms, let $\Delta G_{poly,films}$ equal zero, convert the volumetric energy to a molar formation energy ($\Delta\Delta G_{m,bulk}$), and rearrange terms in Eq. 1 to yield:

$$\Delta\Delta G_{m,bulk} = \gamma_{sub/film}(V_F N_A)/t, \quad (2)$$

where t is the film thickness, V_F is the volume per formula unit (assuming the differences are negligible), and N_A is Avagadro's number.

By tailoring the interface energy to be low (ideally zero) for the targeted metastable phase versus the competitive stable phase, one captures thin nuclei thermodynamically when $\Delta\Delta G_{m,bulk}$ is less than that described in Eq. e:delG-bulk. A typical dioxide formula unit volume is 30 \AA^3 (see 1), a typical nucleation layer is on the order of 1 nm thick (a few formula unit monolayers), and incoherent (coherent) interfacial energies for a stable (metastable) phase are on the order of 1 (0) J/m². Plugging these values into Eq. e:delG-bulk, one finds that $\Delta\Delta G_{m,bulk} \approx 18 \text{ kJ/mol}$. This simple model indicates that a reasonable target window of DFT relative polymorph stabilities is on the order of 10-20 kJ/mol. Some examples are described later, but the SmMnO₃ work described previously had experimentally determined energy differences of $\Delta\Delta G_{m,bulk} \approx 9 \text{ kJ/mol}$, and was only isolated using an isostructural substrate. This observation indicates that 10-20 kJ/mol is a reasonable energetic target window to begin the discussion of epitaxial stabilization, as long as isostructural substrates can be found, which the CSE methodology affords. The absolute window will vary with phase competition, obviously, since the value of $\gamma_{sub/film}$ will vary with polymorph structures and their preferred orientations with the specific substrate. We note that the computational results yield 0 K values of internal energies, while the difference of interest is the synthesis temperature free energy value. In this initial work, we propose that the 0 K values of internal energies are a reasonable starting point for synthetic guidance, though the absolute window will also vary based on how the free energy differences vary with temperature.

3.1 TiO₂

Rutile, anatase and brookite are the naturally occurring polymorphs⁶¹⁻⁶³ of TiO₂, with columbite (often called TiO₂-II) occurring as the first high pressure phase.^{64,65} Thermodynamic studies^{62,66-68} have shown that rutile is the most stable TiO₂ polymorph under ambient conditions. Other studies have reported that the generation of anatase is stabilized kinetically at lower temperatures and smaller particle sizes.⁶⁹⁻⁷¹

The equilibrium energy vs. volume has been plotted for all polymorphs across all func-

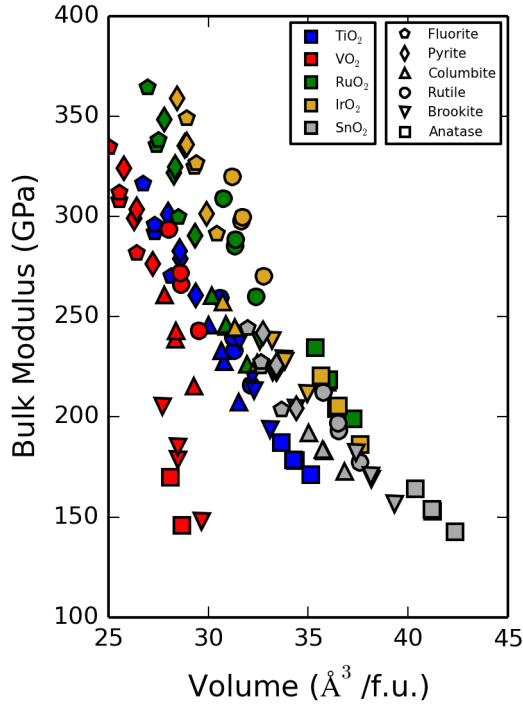


Figure 1: Dependence of bulk modulus on volume for all the polymorphs and compositions considered in this work. Results from all of the exchange-correlation functionals are included in this figure.

tionals in 3 with rutile in each functional as the energy zero. The anatase, brookite, rutile and columbite phases have been found to be almost identical in energy with all of them lying within a maximum of 8 kJ/mol of each other. For the LDA functionals the order of stability has been found to be columbite > brookite > anatase > rutile > pyrite > fluorite. For the GGA functionals, the order is anatase > brookite > columbite > rutile > pyrite > fluorite. Anatase is observed to be more stable than rutile, similar to other theoretical works.^{72–74} To produce better agreement with experiments, corrections in the form of zero-point energies⁶⁸ or DFT+U methods⁷⁴ may have to be considered. The peculiar position of the columbite phase has also been resolved to an extent by Arroyo-de Dompablo et al.⁷⁴ for GGA functionals over a small range of values of the U parameter.

While our results do not address the uncertainty regarding the exact ordering of phase stabilities, they are relevant from a predictive synthesis standpoint. The extremely small en-

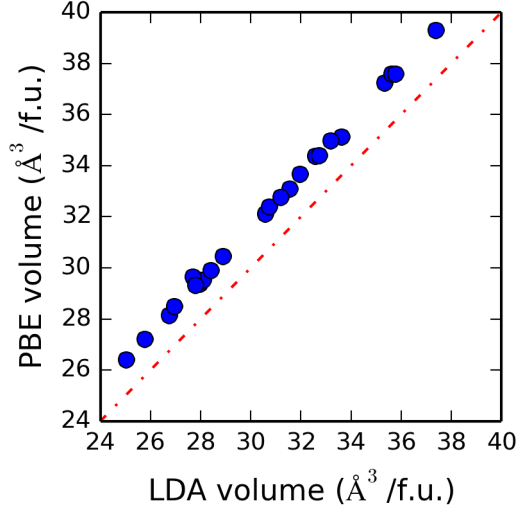


Figure 2: Parity plot of LDA and PBE volumes for all polymorphs of all oxides. The LDA volumes are all observed to be smaller than the PBE volumes.

ergy differences indicate that the phase stability of these polymorphs would be very sensitive to slight changes in synthesis conditions such as pressure, temperature, lattice stresses, etc. This is evidenced by the fact that rutile and anatase can be grown epitaxially,^{21,22,31,75,76} where the substrate controls the formation of a specific phase. Our results indicate that columbite and brookite polymorphs should also be possible to stabilize via epitaxial stabilization, if a suitable substrate can be found. It is known that synthesis conditions can be tailored in atomic layer deposition (ALD) to generate columbite rich TiO_2 films, in direct competition with both the anatase and rutile polymorphs.^{77,78} Additionally, brookite-rich TiO_2 films were fabricated with pulsed laser deposition (PLD) by modifying kinetics from those found to stabilize anatase or rutile.⁷⁹ Recently, Tarre et al. showed that epitaxy modified phase fractions in ALD TiO_2 films, where epitaxial columbite was observed (in the temperature range of 425 – 475 °C) in films on c-sapphire (001) but not on r-sapphire(012), in otherwise identical conditions.⁸⁰

The absence of commercially available substrates that are isostructural with the metastable columbite, brookite, and anatase structures (which would lead to near zero values of $\gamma_{\text{sub/film}}$ for the metastable phases) limit our understanding as to what extent epitaxial stabilization

Table 1: Comparison of a few calculated volumes to theoretical and experimental values

Oxide	Polymorph	V ($\text{\AA}^3/\text{f.u.}$) (this work)	V ($\text{\AA}^3/\text{f.u.}$) (theory)	V ($\text{\AA}^3/\text{f.u.}$) (expt)
TiO ₂	rutile	31.22 (PBEsol)		31.20, ⁵¹ 31.21 ⁵²
		32.11 (PBE)	31.71 (PW91) ⁵³	
	anatase	34.25 (PBEsol)		34.17 ⁵²
		35.13 (PBE)	34.77 (PW91) ⁵³	
	columbite	30.64 (PBEsol)		30.59 ⁵⁴
		31.51 (PBE)	31.18 (PW91) ⁵³	
	pyrite	28.56 (PBEsol)		
		29.36 (PBE)	29.07 (PW91) ⁵³	
VO ₂	rutile	27.30 (PBEsol)		
		28.15 (PBE)	27.94 (PW91) ⁵³	
		29.52 (PBE)	29.691 (PBE) ⁵⁵	
RuO ₂	rutile	31.37 (PBEsol)		31.32 ⁵¹
IrO ₂	rutile	31.19 (LDA)	31.14 (LDA) ⁵⁶	
		32.77 (PBE)	32.89 (GGA) ⁵⁶	
	columbite	30.71 (LDA)	30.68 (LDA) ⁵⁶	
		32.46 (PBE)	32.57 (GGA) ⁵⁶	
	pyrite	28.42 (LDA)	28.40 (LDA) ⁵⁶	
		29.90 (PBE)	30.01 (GGA) ⁵⁶	29.96 ⁵⁷
SnO ₂	rutile	36.48 (PBEsol)		35.73 ⁵¹
	columbite	35.72 (PBEsol)		35.26 ⁵⁸
	pyrite	33.40 (PBEsol)		32.65 ⁵⁹

can be used to direct the synthesis of each of these four polymorphs, or over which thermodynamic conditions (temperature and pressure) the different phases compete. Further experimental and computational investigations are needed to unravel these questions. Nevertheless, these prior observations in film growth clearly indicate that significant room exists for epitaxial stabilization.

Fluorite and pyrite are known to exist in high pressure synthesis, however their relative stabilities with respect to each other vary significantly with the functional used. For the LDA functionals, the energy differences are such that we predict epitaxial driving forces (which is possible using solid phase epitaxy) would considerably influence the phase competition at elevated pressures, but less so considering the GGA functionals (as the volumetric energy differences would swamp interfacial energy contributions).

3.2 VO₂

Vanadium dioxide exists in a large number of polymorphic phases. These include three rutile-type VO₂ (R), monoclinic VO₂ (M),⁸¹ and triclinic VO₂(T)⁸² which are similarly

Table 2: Comparison of a few calculated bulk moduli to theoretical and experimental values

Oxide	Polymorph	Bulk (GPa) (This work)	Modulus	Bulk (GPa) (Theory)	Modulus	Bulk (GPa) (Expt)	Modulus	
TiO ₂	rutile	239.76 (PBEsol)				222,211 ^{51,52}		
		215.78 (PBE)		211 (PW91) ⁵³				
	anatase	178.71 (PBEsol)				179 ⁵²		
		171.42 (PBE)		189 (PW91) ⁵³				
	columbite	233.23 (PBEsol)				260 ⁵⁴		
		207.59 (PBE)		207 (PW91) ⁵³				
pyrite	268.58 (PBE)		250 (PW91) ⁵³					
fluorite	270.33 (PBE)		254 (PW91) ⁵³					
VO ₂	rutile	243.10 (PBE)		248.5 (PBE) ⁵⁵				
RuO ₂	rutile	309.10 (LDA)		299, (LDA) ^{16,60}	297			
		288.43 (PBEsol)				270 ⁵¹		
		259.90 (PBE)		249 (GGA) ¹⁶				
		348.28 (LDA)		346, (LDA) ^{16,60}	339			
	pyrite	290.61 (PBE)		299 (GGA) ¹⁶				
		364.30 (LDA)		351, (LDA) ^{16,60}	345			
		338.06 (PBEsol)				399 ¹⁵		
		299.77 (PBE)		297 (GGA) ¹⁶				
	IrO ₂	rutile	319.80 (LDA)		314.5 (LDA) ⁵⁶			
		rutile	270.36 (PBE)		266.0 (GGA) ⁵⁶			
columbite		257.56 (LDA)		258.7 (LDA) ⁵⁶				
columbite		227.07 (PBE)		231.0 (GGA) ⁵⁶				
pyrite		359.14 (LDA)		352.7 (LDA) ⁵⁶				
pyrite		301.47 (PBE)		297.1 (GGA) ⁵⁶		306 ⁵⁷		
SnO ₂	rutile	197.04 (PBEsol)				205, 224 ^{51,58}		
	columbite	183.81 (PBEsol)				208 ⁵⁸		
	pyrite	241.87 (LDA)				261,252 ^{58,59}		

structured and interconvertible on heating from 325 to 340 K. Several metastable polymorphs are also known, the most common ones being VO₂(A),⁸³ VO₂(B)⁸⁴ and VO₂(C).⁸⁵ Our goal here is to compare the relative stability of other well-known dioxide polymorphs to the stable rutile form of VO₂, to uncover potential targets for epitaxial stabilization. There are few studies of VO₂ polymorph stability in the phases discussed here, as most investigations focus on the behavior of the strongly correlated electrons in the known rutile-related phases (R, M, and T) or ion insertion in the open structured metastable phases. Vanadium oxides can adopt a wide range of V:O ratios, resulting in many different phase competitions over narrow changes in thermodynamic conditions. The vast majority of high-pressure work has also focused on the pressure-driven changes in the rutile-related phases (R, M, and T).

The results shown in 4 indicate that the relative stability of pyrite and fluorite are considerably lower than the same for TiO₂. Columbite and brookite polymorphs have similar

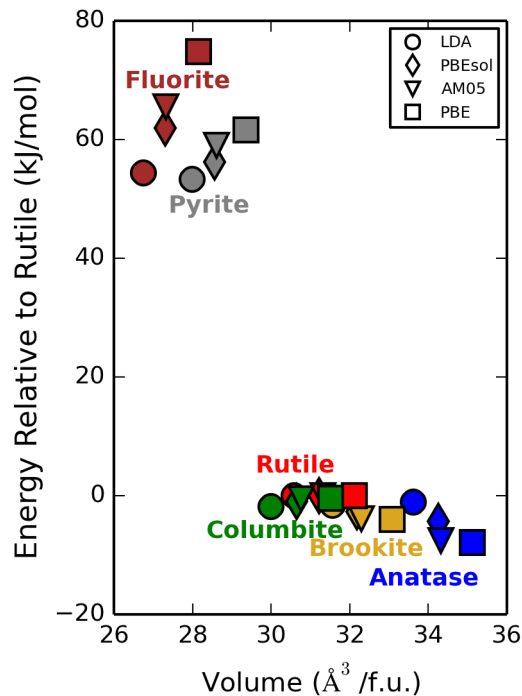


Figure 3: Relative stabilities for TiO_2 polymorphs.

equilibrium energies, around 6-8 kJ/mol more than the rutile polymorph, while anatase is slightly less stable, between 12-16 kJ/mol more than rutile. The anatase results should be interpreted with caution, as the PBE and the AM05 functionals do not produce well-fit equations of state. Further, the volume per formula unit for the anatase polymorph is seen to be quite close to that of rutile VO_2 , which is unusual because anatase generally has a higher volume than rutile for other oxides. These calculations, which are seen as outliers in 1, also indicate that anatase has an unusually low bulk modulus. These calculations were checked for errors, and repeated with different PAW potentials, with similar results.³⁸ Brookite also shows similar behavior, though less pronounced. This might mean that these polymorphs are unstable as bulk phases, but could still be accessible as thin films under strain.

Recent studies on vanadia-titania catalysts indicate that pseudomorphic growth of VO_2 occurred on the (001) and (101) surfaces of anatase TiO_2 ,^{86,87} though only for thicknesses of a few atomic layers. In these studies, VO_2 with a b lattice constant of 3.78 Å has been observed,

which is in agreement with our observed b lattice constant of anatase VO_2 , 3.72 Å for LDA and 3.75 for PBEsol. A DFT study⁸⁸ also indicated that the epitaxial growth of anatase vanadium dioxide, resulting in pseudomorphic VO_2 films. The effect of non-stoichiometry, or varying metal:oxygen ratios, on phase stability is outside the scope of this work, though similar comparisons could be made for varying degrees of non-stoichiometry.

Our results show that the brookite and columbite phases should be accessible by epitaxy, particularly if the anatase polymorph has indeed been stabilized as monolayers, because they compete even better with rutile. The question for synthesis by design is to bracket the relative energy range that can be addressed. For example, it would appear that that range for anatase is on the order of 15-20 kJ/mol, depending on the functional, which falls within our postulated target window. Similar to SmMnO_3 , this could only be done on using isostructural anatase TiO_2 surfaces, owing to the large difference in relative stability (for TiO_2 polymorphs, which have smaller energy differences, one can use non-isostructural surfaces of commercially available crystals). In the case of brookite and columbite polymorphs, much less is known. However, columbite structured films have been successfully grown using epitaxy for TiO_2 ⁸⁰ and SnO_2 ,⁸⁹⁻⁹² both on non-isostructural single crystal substrates, which are not ideal for epitaxial stabilization. For these two oxides, columbite is less than 3-5 kJ/mol less stable than rutile, while columbite VO_2 is only different by 6-8 kJ/mol. Based on these arguments, columbite VO_2 should be accessible using a proper substrate, such as a columbite structured polycrystal using CSE. Since no other brookite structured films are known to the authors, except for TiO_2 , experiments do not help bracket expectations using these 0 K energies. However, using 10-20 kJ/mol as a window, one can postulate that brookite structured films VO_2 should be attainable on certain substrates (such as brookite TiO_2).

3.3 RuO_2

RuO_2 is most commonly observed in the rutile polymorph, and all reports for RuO_2 films focus on and discuss the rutile polymorph. It has also been previously reported that RuO_2

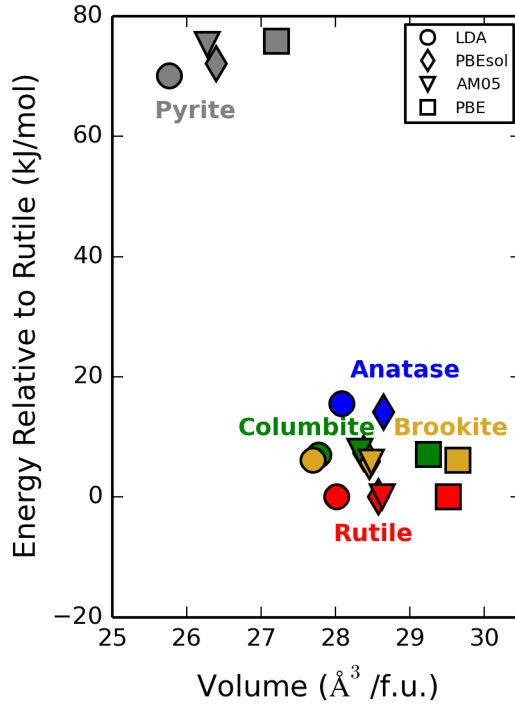


Figure 4: Relative stabilities for VO_2 polymorphs. The fluorite polymorph lies outside the plotted range.

transforms from the rutile polymorph to an orthorhombic CaCl_2 type structure under pressure, before transforming into a cubic polymorph. Initially the cubic polymorph was believed to be fluorite-structured,⁹³ but it has been subsequently shown (experimentally and computationally) to be a pyrite-type polymorph.^{15,16} Our results, shown in 5, also indicate that the pyrite polymorph is considerably more stable than fluorite, by approximately 30 kJ/mol. Since fluorite is more dense, it may be accessible under higher pressures than those investigated; computational predictions place this pressure between 70 and 100 GPa.^{16,60}

Considering the slightly higher volume (i.e., lower pressure) phases, there is no evidence in the literature of the columbite polymorph being formed under pressure, though it is common in other metal dioxides. This can be explained by comparing the ground state energies of pyrite and columbite. It is seen that, for the LDA and PBEsol functionals, the pyrite polymorph is more stable than columbite, while the AM05 functional results in very similar energies. Only results from the PBE functional show that columbite is more stable.

Under pressure, however, pyrite will always be more stable in bulk than columbite. At low pressures, the columbite polymorph is less stable than rutile by approximately 13 kJ/mol for all functionals. In section 3.2, we presented arguments that epitaxial columbite phases have been formed on non-ideal substrates (corundum and fluorite), overcoming at least 5 kJ/mol. Deposition of RuO₂ films on columbite structured under layers, such as α -PbO₂, MgNb₂O₆ and columbite SnO₂, stand as an important test on the utility of epitaxial stabilization to realize metastable columbite films, as 13 kJ/mol is within our proposed 10 - 20 kJ/mol cut-off for the window of DFT energies that can be overcome using epitaxy (the window depends on how the energies actually vary with temperature, which we do not know). In the prior work²⁵ on epitaxially stabilized rare-earth manganites, the experimental enthalpic energy differences at 800 °C were approximately 10 kJ/mol, which is a reasonable minimal cut-off to consider (with the free energy difference being 9 kJ/mol).

Similar arguments hold for pyrite-structured RuO₂, where the range of relative energies are between 5 and 20 kJ/mol, depending on the functional. There are few investigations on epitaxially-stabilized pyrite polymorphs, so it is difficult to use experimental benchmarks as discussed previously for anatase and columbite. Nevertheless, pyrite-structured RuO₂ is a good candidate for epitaxial stabilization, as it has the lowest relative energetic difference of all pyrite phases. Considering the more open volume structures, brookite and anatase, the relative energies are greater than 30 and 50 kJ/mol, respectively, as compared to rutile. It seems unlikely that epitaxial stabilization alone would stabilize them.

3.4 IrO₂

Iridium oxide polymorphs show a similar trend in relative stabilities to the ruthenium oxide polymorphs as a result of the similar bonding character of Ru and Ir, however we find that the relative stability of rutile against all other polymorphs is greater for IrO₂ than for RuO₂ (see 6). Under ambient conditions IrO₂ is known to adopt a rutile-type structure, to which our findings correspond well. The pyrite and columbite are the next two stable

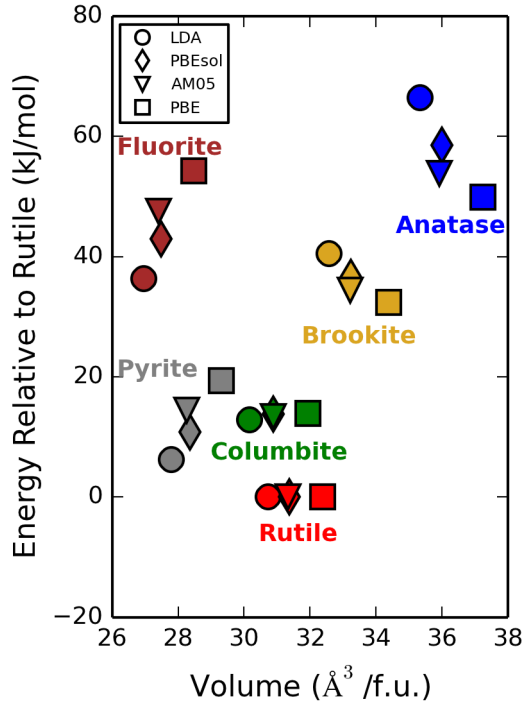


Figure 5: Relative stabilities for RuO_2 polymorphs.

phases, with the order depending on the functional, similar to those of RuO_2 . However, the columbite-structured IrO_2 phase is greater than 20 kJ/mol less stable than rutile, and while the pyrite polymorph stability varies strongly with functional it is greater than 18 kJ/mol. The brookite, anatase, and fluorite (not shown) phases are very unstable compared to rutile. The order of stability for IrO_2 for the LDA, PBEsol and AM05 functionals is rutile > pyrite > columbite > brookite > anatase > fluorite. For the PBE functional the positions of columbite and pyrite are exchanged.

Similar to the RuO_2 polymorphs, the lower ground state energies of the pyrite polymorph compared to the columbite polymorph suggest that the rutile phase will transform to the pyrite phase directly under pressure without forming the columbite phase. This is in agreement with previous experimental findings,^{56,57} where rutile undergoes a phase transition to pyrite at pressures of around 15 GPa. A clear target for epitaxial stabilization would be the pyrite phase, owing to its stability with respect to pressure. Also, should one find that

columbite-structured VO_2 and RuO_2 can be stabilized via epitaxy, columbite IrO_2 would be a natural extension to test the limits of stability.

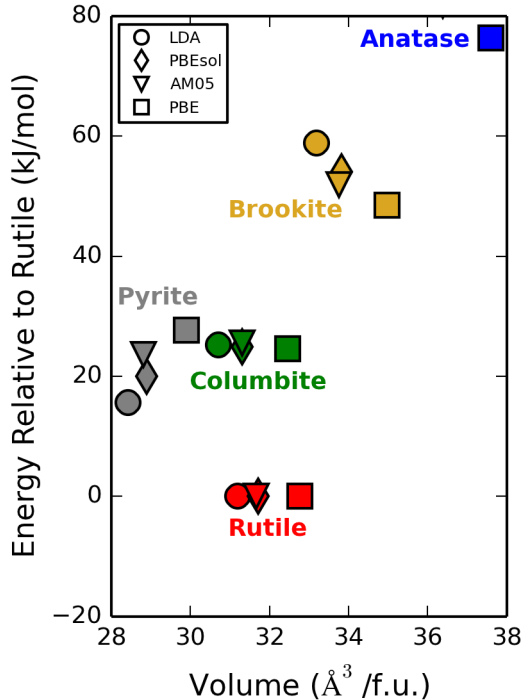


Figure 6: Relative stabilities for IrO_2 polymorphs. The anatase and fluorite polymorphs lie outside the plotted energy range.

3.5 SnO_2

The columbite, brookite, pyrite and anatase polymorphs all lie approximately within 20-30 kJ/mol (see 7) of the most stable polymorph, rutile. This is likely within the feasible range for epitaxial synthesis. The columbite polymorph only differs from the rutile polymorph by around 3 to 5 kJ/mol depending on the functional used. Several high-pressure studies^{15,58,94–96} have reported a rutile-columbite transition pressure of 12 GPa to 21 GPa depending on the method. The small difference also suggests that epitaxial stabilization should be effective in the isolation of the columbite polymorph for SnO_2 . Columbite SnO_2 has been reported as an epitaxial phase, with numerous studies showing that it can be grown as a

thin film.^{89–92,97} Neither the brookite nor the anatase phase have been seen experimentally, although a recent theoretical study⁹⁸ reports an anatase structure with an a -lattice constant of 3.975 Å, similar to our result of 3.982 Å. Since the VO₂ anatase polymorph is difficult to stabilize beyond a few atomic layers, it may be impossible to realize anatase SnO₂, but it certainly warrants investigation using epitaxy. Similarly, the brookite phase lies near the edge of the postulated stability window, warranting investigation using epitaxy.

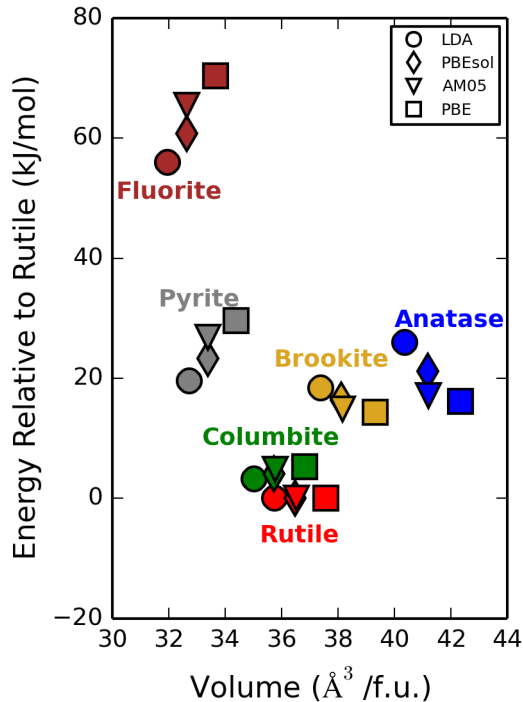


Figure 7: Relative stabilities for SnO₂ polymorphs.

4 Conclusions

We have studied the relative stability of the rutile, anatase, columbite, brookite, pyrite and fluorite polymorphs of five different transition metal oxides: TiO₂, VO₂, RuO₂, IrO₂, SnO₂ with the goal to identify potential targets for epitaxial synthesis. Typical values of BO₂ volumes, film thicknesses and interfacial energies indicate that 10-20 kJ/mol from the most

stable polymorph is a reasonable target window within which epitaxial stabilization should be possible. Previously observed epitaxially stabilized polymorphs like columbite and brookite TiO_2 , anatase VO_2 , and columbite SnO_2 have all been found to lie within this energetic window. With this in mind, our results show that there are many potential candidates for epitaxial synthesis. We have found that the columbite and brookite polymorphs of VO_2 and the pyrite and columbite polymorphs of RuO_2 lie immediately within this window, and are thus prime candidates for epitaxial synthesis. The pyrite and anatase polymorphs of IrO_2 and the brookite and anatase polymorphs of SnO_2 lie towards the edge of the postulated window and should be considered as targets if synthesis efforts of the more feasible candidates are successful. A full list of epitaxial and high pressure targets is given in 3.

Thin film synthesis can be seen as an alternative or complement to high pressure methods. It is especially important where polymorphs cannot be accessible as stable phases under pressure. For example, the columbite polymorph of RuO_2 is metastable over all pressure ranges, but may be stabilized by epitaxy. Epitaxial stabilization can be used to access polymorphs which have similar or higher volumes than the stable ground state polymorph. It is not possible to synthesize these polymorphs using high pressure compression. Anatase VO_2 is an example, having been successfully observed as monolayers over anatase TiO_2 . Anatase SnO_2 and brookite polymorphs of VO_2 and SnO_2 are other high volume epitaxial targets. Finally, we have found that pyrite RuO_2 and IrO_2 , generally considered high-pressure polymorphs, may also be accessible as epitaxial phases.

Our results serve as a starting point for the accelerated discovery of epitaxially stabilized oxide polymorphs. They can be used to guide future efforts focused toward a more comprehensive investigation of the identified growth candidates. These would involve the inclusion of strain effects induced by epitaxy, selection of appropriate substrates, the estimation of the interfacial energy between the film and the substrate, and the surface energy of the free surface. There are still substantial challenges involved in the development of epitaxial stabilization for the development of new materials, but initial results merit further computational

and experimental activity.

Table 3: Potential Epitaxial and High Pressure Targets

Oxide	Ambient Polymorph	Epitaxial Targets	High Pressure Targets
TiO ₂	Anatase, Rutile	Columbite, Brookite	Pyrite, Fluorite
VO ₂	Rutile	Columbite, Brookite, Anatase	Pyrite
RuO ₂	Rutile	Pyrite, Columbite	Pyrite, Fluorite
IrO ₂	Rutile	Pyrite, Columbite	Pyrite
SnO ₂	Rutile	Columbite, Brookite, Anatase	Pyrite, Fluorite

Acknowledgement

JRK gratefully acknowledges support from the DOE Office of Science Early Career Research Program (DE-SC0004031).

Supporting Information Available: All of the data files used in this work, including examples of how to use it are in the Supporting Information. This information is available free of charge via the Internet at <http://pubs.acs.org>.

5 References

References

- (1) Shapovalov, V.; Metiu, H. *Journal of Catalysis* **2007**, *245*, 205–214.
- (2) Chrétien, S.; Metiu, H. *Catalysis Letters* **2006**, *107*, 143–147.
- (3) Busca, G.; Lietti, L.; Ramis, G.; Berti, F. *Applied Catalysis B: Environmental* **1998**, *18*, 1–36.
- (4) Over, H.; Muhler, M. *Progress in Surface Science* **2003**, *72*, 3–17.
- (5) Linsebigler, A. L.; Lu, G.; Yates, J. T. *Chemical Reviews* **1995**, *95*, 735–758.
- (6) Osterloh, F. E. *Chemistry of Materials* **2008**, *20*, 35–54.

- (7) Hardee, K. L.; Bard, A. J. *Journal of The Electrochemical Society* **1977**, *124*, 215–224.
- (8) Feng, Y.; Li, X. *Water Research* **2003**, *37*, 2399–2407.
- (9) Meixner, H.; Lampe, U. *Sensors and Actuators B: Chemical* **1996**, *33*, 198–202.
- (10) Korotcenkov, G. *Materials Science and Engineering B* **2007**, *139*, 1–23.
- (11) Strukov, D. B.; Snider, G. S.; Stewart, D. R.; Williams, R. S. *Nature* **2008**, *453*, 80–83.
- (12) Waser, R.; Aono, M. *Nature Materials* **2007**, *6*, 833–840.
- (13) Hadjiivanov, K. I.; Klissurski, D. G. *Chemical Society Reviews* **1996**, *25*, 61–69.
- (14) Sclafani, A.; Herrmann, J. M. *The Journal of Physical Chemistry* **1996**, *100*, 13655–13661.
- (15) Haines, J.; Léger, J. M.; Schulte, O. *Science* **1996**, *271*, pp. 629–631.
- (16) Tse, J. S.; Klug, D. D.; Uehara, K.; Li, Z. Q.; Haines, J.; Léger, J. M. *Physical Review B* **2000**, *61*, 10029–10034.
- (17) Liu, H.; Wang, Y.; Wang, K.; Hosono, E.; Zhou, H. *Journal of Materials Chemistry* **2009**, *19*, 2835–2840.
- (18) Posadas, A.; Yau, J.-B.; Ahn, C. H.; Han, J.; Gariglio, S.; Johnston, K.; Rabe, K. M.; Neaton, J. B. *Applied Physics Letters* **2005**, *87*, 171915.
- (19) Liu, J. Z.; Zunger, A. *Journal of Physics: Condensed Matter* **2009**, *21*, 295402.
- (20) Stampfl, C.; Freeman, A. *Applied Surface Science* **2012**, *258*, 5638–5645.
- (21) Silva, V. F.; Bouquet, V.; Députier, S.; Boursicot, S.; Ollivier, S.; Weber, I. T.; Silva, V. L.; Santos, I. M. G.; Guilloux-Viry, M.; Perrin, A. *Journal of Applied Crystallography* **2010**, *43*, 1502–1512.

- (22) Zhang, Y.; Schultz, A. M.; Salvador, P. A.; Rohrer, G. S. *Journal of Materials Chemistry* **2011**, *21*, 4168–4174.
- (23) Atsumi, T.; Ohgushi, T.; Kamegashira, N. *Journal of Alloys and Compounds* **1996**, *238*, 35–40.
- (24) Balasubramaniam, K. R. Thin film growth and phase competition of layered ferro-electrics and related perovskite phases. Ph.D. thesis, Carnegie Mellon University, 2006.
- (25) Balasubramaniam, K. R.; Havelia, S.; Salvador, P. A.; Zheng, H.; Mitchell, J. F. *Applied Physics Letters* **2007**, *91*, 232901.
- (26) Zhang, Y.; Schultz, A. M.; Li, L.; Chien, H.; Salvador, P. A.; Rohrer, G. S. *Acta Materialia* **2012**, *60*, 6486–6493.
- (27) Havelia, S.; Wang, S.; Balasubramaniam, K. R.; Schultz, A. M.; Rohrer, G. S.; Salvador, P. A. *CrystEngComm* **2013**, *15*, 5434–5441.
- (28) Havelia, S.; Wang, S.; Balasubramaniam, K. R.; Salvador, P. A. *Crystal Growth & Design* **2009**, *9*, 4546–4554.
- (29) Schultz, A. M.; Zhu, Y.; Bojarski, S. A.; Rohrer, G. S.; Salvador, P. A. *Thin Solid Films* **2013**, *548*, 220–224.
- (30) Pravarthana, D.; Lebedev, O. I.; Hebert, S.; Chateigner, D.; Salvador, P. A.; Prellier, W. *Applied Physics Letters* **2013**, *103*, 143123.
- (31) Burbure, N. V.; Salvador, P. A.; Rohrer, G. S. *Chemistry of Materials* **2010**, *22*, 5823–5830.
- (32) Ahuja, R.; Rekhi, S.; Saxena, S.; Johansson, B. *Journal of Physics and Chemistry of Solids* **2001**, *62*, 2035 – 2037.

- (33) Dubrovinskaia, N. A.; Dubrovinsky, L. S.; Ahuja, R.; Prokopenko, V. B.; Dmitriev, V.; Weber, H. P.; Osorio-Guillen, J. M.; Johansson, B. *Physical Review Letters* **2001**, *87*, 275501.
- (34) Manjón, F. J.; Errandonea, D. *physica status solidi (b)* **2009**, *246*, 9–31.
- (35) Gorbenko, O. Y.; Samoilenov, S. V.; Graboy, I. E.; Kaul, A. R. *Chemistry of Materials* **2002**, *14*, 4026–4043.
- (36) Jain, A.; Ong, S. P.; Hautier, G.; Chen, W.; Richards, W. D.; Dacek, S.; Cholia, S.; Gunter, D.; Skinner, D.; Ceder, G.; Persson, K. A. *APL Materials* **2013**, *1*, 011002.
- (37) de-la Roza, A. O.; Abbasi-Pérez, D.; na, V. L. *Computer Physics Communications* **2011**, *182*, 2232–2248.
- (38) Supporting information.
- (39) Kresse, G.; Furthmüller, J. *Computational Materials Science* **1996**, *6*, 15–50.
- (40) Kresse, G.; Furthmüller, J. *Physical Review B* **1996**, *54*, 11169–11186.
- (41) Blöchl, P. E. *Physical Review B* **1994**, *50*, 17953–17979.
- (42) Kresse, G.; Joubert, D. *Physical Review B* **1999**, *59*, 1758–1775.
- (43) Perdew, J. P.; Zunger, A. *Physical Review B* **1981**, *23*, 5048–5079.
- (44) Perdew, J. P.; Burke, K.; Ernzerhof, M. *Physical Review Letters* **1996**, *77*, 3865–3868.
- (45) Perdew, J. P.; Burke, K.; Ernzerhof, M. *Physical Review Letters* **1997**, *78*, 1396–1396.
- (46) Perdew, J. P.; Ruzsinszky, A.; Csonka, G. I.; Vydrov, O. A.; Scuseria, G. E.; Constantin, L. A.; Zhou, X.; Burke, K. *Physical Review Letters* **2008**, *100*, 136406.
- (47) Armiento, R.; Mattsson, A. E. *Physical Review B* **2005**, *72*, 085108.

- (48) Mattsson, A. E.; Armiento, R.; Paier, J.; Kresse, G.; Wills, J. M.; Mattsson, T. R. *Journal of Chemical Physics* **2008**, *128*, 084714.
- (49) Monkhorst, H. J.; Pack, J. D. *Physical Review B* **1976**, *13*, 5188–5192.
- (50) Hebbache, M.; Zemzemi, M. *Physical Review B* **2004**, *70*, 224107.
- (51) Hazen, R. M.; Finger, L. W. *Journal of Physics and Chemistry of Solids* **1981**, *42*, 143–151.
- (52) Burdett, J. K.; Hughbanks, T.; Miller, G. J.; Richardson, J. W.; Smith, J. V. *Journal of the American Chemical Society* **1987**, *109*, 3639–3646.
- (53) Ma, X. G.; Liang, P.; Miao, L.; Bie, S. W.; Zhang, C. K.; Xu, L.; Jiang, J. J. *physica status solidi (b)* **2009**, *246*, 2132–2139.
- (54) Gerward, L.; Staun Olsen, J. *Journal of Applied Crystallography* **1997**, *30*, 259–264.
- (55) Reeswinkel, T.; Music, D.; Schneider, J. M. *Journal of Physics: Condensed Matter* **2009**, *21*, 145404.
- (56) Ono, S.; Brodholt, J. P.; Price, G. D. *Journal of Physics: Condensed Matter* **2008**, *20*, 045202.
- (57) Ono, S.; Kikegawa, T.; Ohishi, Y. *Physica B-Condensed Matter* **2005**, *363*, 140–145.
- (58) Haines, J.; Léger, J. M. *Physical Review B* **1997**, *55*, 11144–11154.
- (59) Ono, S.; Ito, E.; Katsura, T.; Yoneda, A.; Walter, M. J.; Urakawa, S.; Utsumi, W.; Funakoshi, K. *Physics and Chemistry of Minerals* **2000**, *27*, 618–622.
- (60) Hugosson, H. W.; Grechnev, G. E.; Ahuja, R.; Helmersson, U.; Sa, L.; Eriksson, O. *Physical Review B* **2002**, *66*, 174111.

- (61) Ding, X. Z.; Liu, X. H.; He, Y. Z. *Journal of Materials Science Letters* **1996**, *15*, 1789–1791.
- (62) Smith, S. J.; Stevens, R.; Liu, S.; Li, G.; Navrotsky, A.; Boerio-Goates, J.; Woodfield, B. F. *American Mineralogist* **2009**, *94*, 236–243.
- (63) Ghosh, T. B.; Dhabal, S.; Datta, A. K. *Journal of Applied Physics* **2003**, *94*, 4577–4582.
- (64) McQueen, R. G.; Jamieson, J. C.; Marsh, S. P. *Science* **1967**, *155*, 1401–1404.
- (65) Arlt, T.; Bermejo, M.; Blanco, M. A.; Gerward, L.; Jiang, J. Z.; Staun Olsen, J.; Recio, J. M. *Physical Review B* **2000**, *61*, 14414–14419.
- (66) Navrotsky, A.; Kleppa, O. J. *Journal of the American Ceramic Society* **1967**, *50*, 626–626.
- (67) Mitsuhashi, T.; Kleppa, O. J. *Journal of the American Ceramic Society* **1979**, *62*, 356–357.
- (68) Mei, Z. G.; Wang, Y.; Shang, S. L.; Liu, Z.-K. *Inorganic Chemistry* **2011**, *50*, 6996–7003.
- (69) Zhang, H.; Banfield, J. F. *The Journal of Physical Chemistry B* **2000**, *104*, 3481–3487.
- (70) Okada, K.; Yamamoto, N.; Kameshima, Y.; Yasumori, A.; MacKenzie, K. J. D. *Journal of the American Ceramic Society* **2001**, *84*, 1591–1596.
- (71) Shin, H.; Jung, H. S.; Hong, K. S.; Lee, J. K. *Journal of Solid State Chemistry* **2005**, *178*, 15–21.
- (72) Muscat, J.; Swamy, V.; Harrison, N. M. *Physical Review B* **2002**, *65*, 224112.
- (73) Ma, X. G.; Liang, P.; Miao, L.; Bie, S. W.; Zhang, C. K.; Xu, L.; Jiang, J. J. *physica status solidi (b)* **2009**, *246*, 2132–2139.

- (74) Arroyo-de Dompablo, M. E.; Morales-García, A.; Taravillo, M. *Journal of Chemical Physics* **2011**, *135*, 054503–054503–9.
- (75) Schuisky, M.; Hårsta, A.; Aidla, A.; Kukli, K.; Kiisler, A.-A.; Aarik, J. *Journal of The Electrochemical Society* **2000**, *147*, 3319–3325.
- (76) Miao, L.; Tanemura, S.; Jin, P.; Kaneko, K.; Terai, A.; Nabatova-Gabain, N. *Journal of Crystal Growth* **2003**, *254*, 100–106.
- (77) Aarik, J. *Philosophical Magazine Letters* **1996**, *73*, 115–119.
- (78) Aarik, J.; Aidla, A.; Sammelselg, V.; Uustare, T. *Journal of Crystal Growth* **1997**, *181*, 259 – 264.
- (79) Moret, M. P.; Zallen, R.; Vijay, D. P.; Desu, S. B. *Thin Solid Films* **2000**, *366*, 8–10.
- (80) Tarre, A.; Möldre, K.; Niilisk, A.; Mändar, H.; Aarik, J.; Rosental, A. *Journal of Vacuum Science & Technology A* **2013**, *31*, 01A118.
- (81) Morin, F. J. *Physical Review Letters* **1959**, *3*, 34–36.
- (82) Mitsuishi, T. *Japanese Journal of Applied Physics* **1967**, *6*, 1060–1071.
- (83) Oka, Y.; Yao, T.; Yamamoto, N. *Journal of Solid State Chemistry* **1990**, *86*, 116–124.
- (84) Théobald, F.; Cabala, R.; Bernard, J. *Journal of Solid State Chemistry* **1976**, *17*, 431–438.
- (85) Hagrman, D.; Zubieta, J.; Warren, C. J.; Meyer, L. M.; Treacy, M. M.; Haushalter, R. C. *Journal of Solid State Chemistry* **1998**, *138*, 178–182.
- (86) Gao, W.; Wang, C.; Wang, H.; Henrich, V.; Altman, E. *Surface Science* **2004**, *559*, 201–213.
- (87) Gao, W.; Altman, E. *Surface Science* **2006**, *600*, 2572–2580.

- (88) Vittadini, A.; Casarin, M.; Sami, M.; Selloni, A. *The Journal of Physical Chemistry B* **2005**, *109*, 21766–21771.
- (89) Prodan, A.; Vene, N.; sek, F. S.; Hudomalj, M. *Thin Solid Films* **1987**, *147*, 313–319.
- (90) Lamelas, F. J.; Reid, S. A. *Physical Review B* **1999**, *60*, 9347–9352.
- (91) Kong, L.; Ma, J.; Luan, C.; Zhu, Z. *Applied Physics Letters* **2011**, *98*, 261904.
- (92) Kim, S.; Kim, D. H.; Hong, S. H. *Journal of Crystal Growth* **2012**, *348*, 15–19.
- (93) Haines, J.; Léger, J. M. *Physical Review B* **1993**, *48*, 13344–13350.
- (94) Ono, S.; Funakoshi, K.; Nozawa, A.; Kikegawa, T. *Journal of Applied Physics* **2005**, *97*, 073523.
- (95) Shieh, S. R.; Kubo, A.; Duffy, T. S.; Prakapenka, V. B.; Shen, G. *Physical Review B* **2006**, *73*, 014105.
- (96) Gracia, L.; Beltrán, A.; Andrés, J. *The Journal of Physical Chemistry B* **2007**, *111*, 6479–6485.
- (97) Kong, L.; Ma, J.; Zhu, Z.; Luan, C.; Yu, X.; Yu, Q. *Materials Letters* **2010**, *64*, 1350–1353.
- (98) Dou, M.; Persson, C. *Journal of Applied Physics* **2013**, *113*, 083703.